

Reaction of Canine Plasminogen with 6-Aminohexanoate: A Thermodynamic Study Combining Fluorescence, Circular Dichroism, and Isothermal Titration Calorimetry[†]

Jack A. Kornblatt,^{*,‡} Isabelle Rajotte,[‡] and Frédéric Heitz[§]

Enzyme Research Group, Concordia University, 1455 de Maisonneuve Ouest, Montreal, Quebec, Canada H3G 1M8, and CRBM, CNRS, 1919, route de Mende, 34293 Montpellier, France

Received August 8, 2000; Revised Manuscript Received January 9, 2001

ABSTRACT: The thermodynamics of the binding of 6-aminohexanoate (6-AH) to dog glu-plasminogen has been studied. Fluorescence titrations revealed four binding sites. Three yielded positive fluorescence changes on ligand binding; one yielded a negative fluorescence change. The fluorescence data gave no indication of cooperative interactions. Binding was studied using circular dichroism (CD). Near 295 nm there were small changes associated with binding ligand. These were magnified at 235 nm, a wavelength that is mainly associated with tryptophan bands. The dissociation constants obtained from the fluorescence were applied to the CD data and fit quite well. Below 220 nm, there were no significant differences between samples with or without 6-AH and, therefore, no substantial change in the secondary structure of the protein. Isothermal titration calorimetry was used in combination with the binding constants from fluorescence to study the enthalpy and entropy contributions to 6-AH binding. The enthalpies of association for the four sites are all negative. Their absolute values are small for the tight sites and large for the weakest. $-T\Delta S$ is negative for the tight sites and positive for the weakest. The binding of 6-AH to plasminogen is entropically driven for the two tightest sites and enthalpically driven for the weakest site. The binding of 6-AH to lys-plasminogen has been studied and differs slightly from binding to glu-plasminogen. Most importantly, the binding of 6-AH for the weak site goes from enthalpy- to entropy-driven as is found with the other sites.

Among the leading causes of death in Northern Europe and North America are heart disease and stroke. Fibrin clots that form in the peripheral circulation are dislodged from their sites of origin and move to the heart or brain where they cut off the blood and oxygen supplies; the result is stroke if the clot is in the brain and a myocardial infarct if it is in the heart. Plasminogen, the inactive precursor of the fibrinolytic protein plasmin, gives rise to plasmin and thereby helps to reduce the incidence of these events (1).

Plasminogen is a 791-residue peptide composed of seven different and reasonably well characterized domains (2): the N-terminal peptide (NTP)¹ of ~80 amino acids is followed by five kringle domains of 80–90 residues each; these are in turn followed by the carboxy-terminal preproteolytic domain. Intact plasminogen is a closed structure in which lysine 50 of the NTP is noncovalently ligated to a binding

site on kringle 5 (3–5). On the basis of the crystal structures of kringle 5, the site consists of a V-like structure formed from one tryptophan and one tyrosine (6). One extreme of the binding site contains negative charge which can form ion pairs with the positively charged ϵ -amino of lysine 50. The crystal structures of microplasmin as well as four of the five kringles have been determined (6–12).

Of the five kringles of plasminogen, four (expressed as single domains) will bind the NTP (13) even though only kringle 5 binds it in the intact protein. The four kringles, both in the individually expressed domains and in the intact protein, will also bind 6-AH which presumably resembles lysine 50 or the natural binding sites on the target fibrin. Three of these kringles (1, 2, and 4) bind 6-AH quite tightly; the three have a negative charge in the same position as kringle 5 but also have a positive charge at the other extreme of the binding site. This positive charge forms an ion pair with carboxylate of omega amino acids of the correct length.

When plasminogen binds fibrin or 6-AH, lysine 50 is displaced from its position on kringle 5 (3, 4). This produces a large conformational change as the closed form opens; this conformational change is the first step in the activation mechanism to plasmin. The conformational change has been quantified using sedimentation analysis (14–16), circular dichroism (15), fluorescence polarization (17), small-angle X-ray and neutron scattering (18, 19), electron microscopy (20, 21), and gel electrophoresis (22).

Plasminogen responds to high hydrostatic pressure which also causes the molecule to open (22). Lysine 50 is displaced

[†] Supported by the Natural Science and Engineering Research Council of Canada.

* Corresponding author. Telephone: (514) 848-3404. Fax: (514) 848-2881. E-mail: kornblatt@vax2.concordia.ca.

[‡] Concordia University.

[§] CNRS.

¹ Abbreviations: DPGN, canine plasminogen; glu-plasminogen, full-length plasminogen consisting of ~791 amino acids; lys-plasminogen, truncated plasminogen in which residues 1–76, 1–77, or 1–78 have been proteolytically removed; 6-AH, 6-aminohexanoate; NTP, N-terminal peptide; Φ , fluorescence value; CD, circular dichroism. Kringle 1 is the same as site 2, the second tightest 6-AH binding site. Kringle 2 is the same as site 3, the third tightest site. Kringle 3 does not bind 6-AH. Kringle 4 is the same as the tightest binding site, site 1. Kringle 5 is the same as the weakest site (site 4); it is also the binding site for the NTP in the intact protein.

from its site on kringle 5; the driving force for this is, at least in part, ligand replacement with water and electrostriction of the free amino of lysine 50 instead of ligand replacement with 6-AH.

In this report, we show using intrinsic fluorescence, circular dichroism, and isothermal titration calorimetry that the binding of 6-AH by plasminogen can be analyzed as the sum of four hyperbolic functions, each of which represents one of the four binding kringles. The binding constants so obtained have been used to extract the binding entropies and enthalpies from isothermal titration calorimetric experiments. In the intact plasminogen, binding of 6-AH to the two tightest binding kringles is entropically driven. In contrast, binding to the fourth site and the conformational change that results from the binding are enthalpy-driven. This situation applies only in glu-plasminogen, where the NTP is intact. In lys-plasminogen, the NTP has been cleaved between positions 77 and 78 (23); there is no longer any ligation between lysine 50 and kringle 5, and any conformational change that takes place when 6-AH binds to kringle 5 is minor compared to the intact protein (4). In lys-plasminogen, the binding of 6-AH to kringle 5 resembles the binding of 6-AH to the other three kringles in that it is largely entropically driven.

We note that the vast majority of work currently done on plasminogen is performed on human plasminogen and most of that is done on the recombinant protein expressed in tissue culture cells (4, 24, 25). We have elected to study dog plasminogen because the protein is readily available and easily prepared, because it is free from known human pathogens, because its sequence is homologous to that of the human protein (26, 27), and because it may yield useful crystals for structure determination whereas the human protein has not yet done so.

MATERIALS AND METHODS

Plasminogen was purified from frozen dog plasma; the approach (28) was to thaw 100 mL of frozen plasma, pass it through a column containing about 1 mL of lysine sepharose, wash with 0.3 M potassium phosphate (Fluka) (pH 7.4) containing 10 μ M aprotinin (Sigma), and elute with about 2 mL of 5 mM 6-AH (Fluka) in 0.3 M potassium phosphate (pH 7.4). The sample was then simultaneously concentrated and "dialyzed" with Centricon 30 filters such that the 6-AH was diluted to a maximum of 0.5 μ M. Analysis of the dialyzed, concentrated protein showed that it contained less than 0.5 6-AH molecule per DPGN. The final buffer was 25 mM Mes (Boehringer-Mannheim), 25 mM Tris (Sigma), 1 mM magnesium acetate (Fisher), and 0.1 mM EDTA (Fluka) (pH 6.5). The preparation of the purified plasminogen took less than 4 h; the concentration-dialysis step took about the same length of time. The purified plasminogen was divided into aliquots of \sim 0.2 mL containing \sim 0.2 mg of protein and freeze-dried. The dried powder was kept under vacuum at room temperature and was stable over a period of months. In preparation for fluorescence experiments, the dried powder was reconstituted to the original volume with water and then diluted with the Mes/Tris/Mg/EDTA buffer. In most instances, it was used within 2 h for the fluorescence titration. On days when we performed more than one experiment, the plasminogen was kept on ice until the second titration was performed. At the end of every titration, a sample was taken for SDS-PAGE

and assayed for cleaved products. If there was any visible formation of lys-plasminogen or plasmin, the data from the titration were discarded. In preparation for CD experiments, the dried powder was reconstituted with 10 mM disodium phosphate and 10 mM monopotassium phosphate (pH 6.8). Lys-plasminogen was prepared from glu-plasminogen. The original purified glu-plasminogen was diluted with 25% glycerol and stored at 253 K for at least six months, during which time it converted to the lys-plasminogen. We could easily distinguish between the glu and lys forms on 7% SDS-PAGE. The glu-plasminogen runs more slowly than phosphorylase *b*, while the lys-plasminogen runs slightly faster. Our glu-plasminogen preparation contained neither detectable lys-plasminogen, assayed by SDS-PAGE, nor plasmin, assayed by SDS-PAGE and enzymatically with the substrate Chromozym (Boehringer-Mannheim). The lys-plasminogen preparation contained >95% lys-plasminogen and no detectable plasmin.

Fluorometric titrations were carried out at 288 K using a Shimadzu RF-5000 spectrofluorometer with a built-in stirrer or an Aminco Bowman Series 2 luminescence spectrometer equipped with a built-in stirrer. Samples were contained in standard 4 mL quartz cuvettes that contained a heavy-duty stirring bar designed for cuvettes (VWR catalog no. 58949-030, also available from Sigma). Every titration series followed the same procedure.

The samples were stirred for 30 s; the stirring was turned off, and the fluorescence was monitored at 280 (excitation) and 360 nm (emission) for 30 s. This was repeated 10 times to assess photodamage. Two microliters of water was added using a Hamilton syringe equipped with a Chaney adapter; the sample was stirred during the addition, the stirring stopped, and fluorescence monitored for 30 s. This was repeated 10 times to further assess photodamage. Over the course of 20×30 s, the extent of photodamage was <1% of the total fluorescence; a linear correction was applied to the subsequent data. Aliquots of 6-AH (2 μ L) were added with stirring; the stirring was stopped and the fluorescence monitored over the course of 30 s. The concentration of 6-AH in the syringe varied from 2 mM up to 0.5 M. The lowest concentration was used to obtain data on the tight sites, while the higher concentrations gave data that could be applied to the two weaker sites. The fluorescence data were treated using SigmaPlot 5.0.

Circular dichroism was performed on a Jasco model 810 polarimeter using 1 mm rectangular cells. The sample chamber was thermostated at 288 K.

Isothermal titration calorimetry was carried out using a Microcal VP-ITC microcalorimeter maintained at 288 K. The concentration of protein in the titration cell varied from 2 to 10 μ M. The concentration of 6-AH in the injection syringe was \sim 0.5 M. The dissociation constants obtained from the fluorescence titrations were used to extract the entropies and enthalpies for the four binding sites.

RESULTS

Figure 1A shows a complete titration curve with data extending to 25 mM; there was no evidence of additional binding sites at concentrations of >25 mM. Figure 1B shows the same data but emphasizes the region between 0 and 2 mM 6-AH. The data (●) were fit to the sum of four

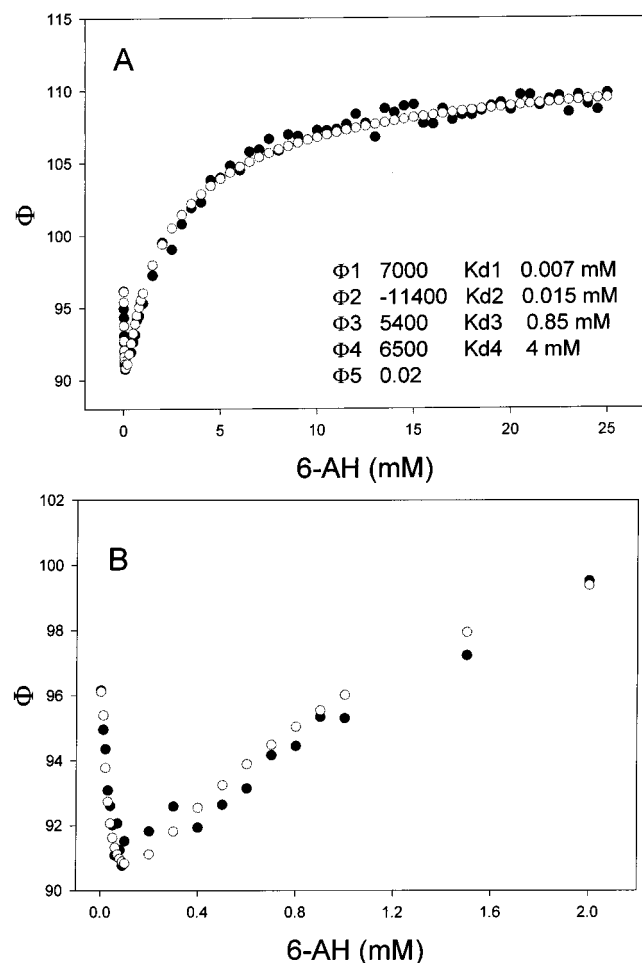


FIGURE 1: Intrinsic fluorescence response of glu-DPGN to the addition of 6-AH. (A) The concentration of glu-DPGN was 2 μ M; the concentration of 6-AH varied from 10 μ M to 25 mM. The black circles are the actual data points; the white circles are data fit to the equation shown in the Results. $T = 288$ K. The buffer contained 25 mM Mes, 25 mM Tris, 1 mM Mg(OAc)₂, and 0.1 mM EDTA (pH 6.5). The fluorescence coefficients and the dissociation coefficients are given in the inset. (B) The same data but emphasizing data between 10 μ M and 2 mM 6-AH.

rectangular hyperbolas using the regression function in Sigma Plot and then further refined by simulating the data with the following equation:

$$\Phi = \Phi_{\text{initial}} + \frac{[\text{DPGN}][6\text{-AH}]\Phi_1}{([\text{6-AH}] + K_{d1})} + \frac{[\text{DPGN}][6\text{-AH}]\Phi_2}{([\text{6-AH}] + K_{d2})} + \frac{[\text{DPGN}][6\text{-AH}]\Phi_3}{([\text{6-AH}] + K_{d3})} + \frac{[\text{DPGN}][6\text{-AH}]\Phi_4}{([\text{6-AH}] + K_{d4})} + ([6\text{-AH}]\Phi_5)$$

where Φ is the fluorescence yield, [DPGN] is the concentration of DPGN, [6-AH] is the concentration of 6-AH, $\Phi_1 - \Phi_4$ are the fluorescence coefficients associated with the binding of 6-AH to that site, and $K_{d1} - K_{d4}$ are the dissociation coefficients associated with binding to the site. (While the protein contains five kringles, kringle 3 does not bind 6-AH in HPGN and presumably does not do so in DPGN.) Φ_5 is a linear term that accounts for very small increases that occur as 6-AH is added; it is independent of DPGN. The global fitting routine allows all sites to be filled at a rate proportional to their respective K_d values. In Figure 1, the black circles are the actual data points while the white circles represent

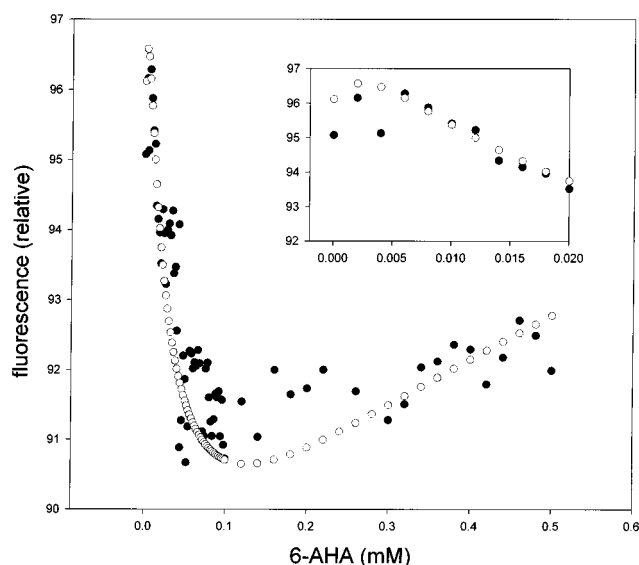


FIGURE 2: Intrinsic fluorescence response of glu-DPGN to the addition of 6-AH. The concentration of DPGN was 2 μ M, and the concentration of 6-AH varied between 2 and 500 μ M. $T = 288$ K; the buffer was the same as that used in Figure 1. The data were fit to the same fluorescence coefficients and dissociation coefficients as used in Figure 1. Black circles are the actual data points; white circles are the fitted points. The inset shows the same data but emphasizes the region between 0 and 20 μ M 6-AH.

fitted values. Where, at any given concentration of 6-AH, there is only a white circle, it means that the actual and fitted points are superimposed. The individual fluorescence coefficients and K_d values are shown in the top panel of Figure 1.

The fits in panels A and B of Figure 1 are not bad, but they are not perfect. The scatter in the data is such that perfect fits will not be obtained. It is essential to point out that there is no unique fit to the data of Figure 1. With four dissociation constants and four fluorescence coefficients, the data can be approximated with many combinations. We can say that the data were also fit to the sum of two and three hyperbolic functions; the fits were very much poorer. Four-factor Hill plots, three-factor Hill plots, and two-factor Hill plots also gave poor fits over the entire titration range. If it is considered that there are four known binding sites in plasminogen, the use of four sets of coefficients is probably justified (see the Discussion). The experiment whose results are depicted in Figure 1 has been repeated more than 10 times with effectively the same results.

Figure 2 shows a fluorescence titration curve using a different sample on a different day. Here we titrated the DPGN with 6-AH but stopped after reaching 0.5 mM. The inset emphasizes the curve between 0 and 20 μ M 6-AH. About 70 points were taken in the concentration range from 0 to 0.5 mM. There is scatter in the data; it is especially noticeable in the region around 0.07 mM because the fluorescence changes are so small and because there are many points in this region. The data points (●) were fitted (○) using the fluorescence coefficients and K_d values shown in Figure 1. Once again, the coefficients obtained from the fitting routine give acceptable but not perfect correlations with the actual data.

Figure 3 shows the results of similar titrations monitoring the samples with circular dichroism. Panel A demonstrates the changes in the range from 310 to 220 nm, whereas panel

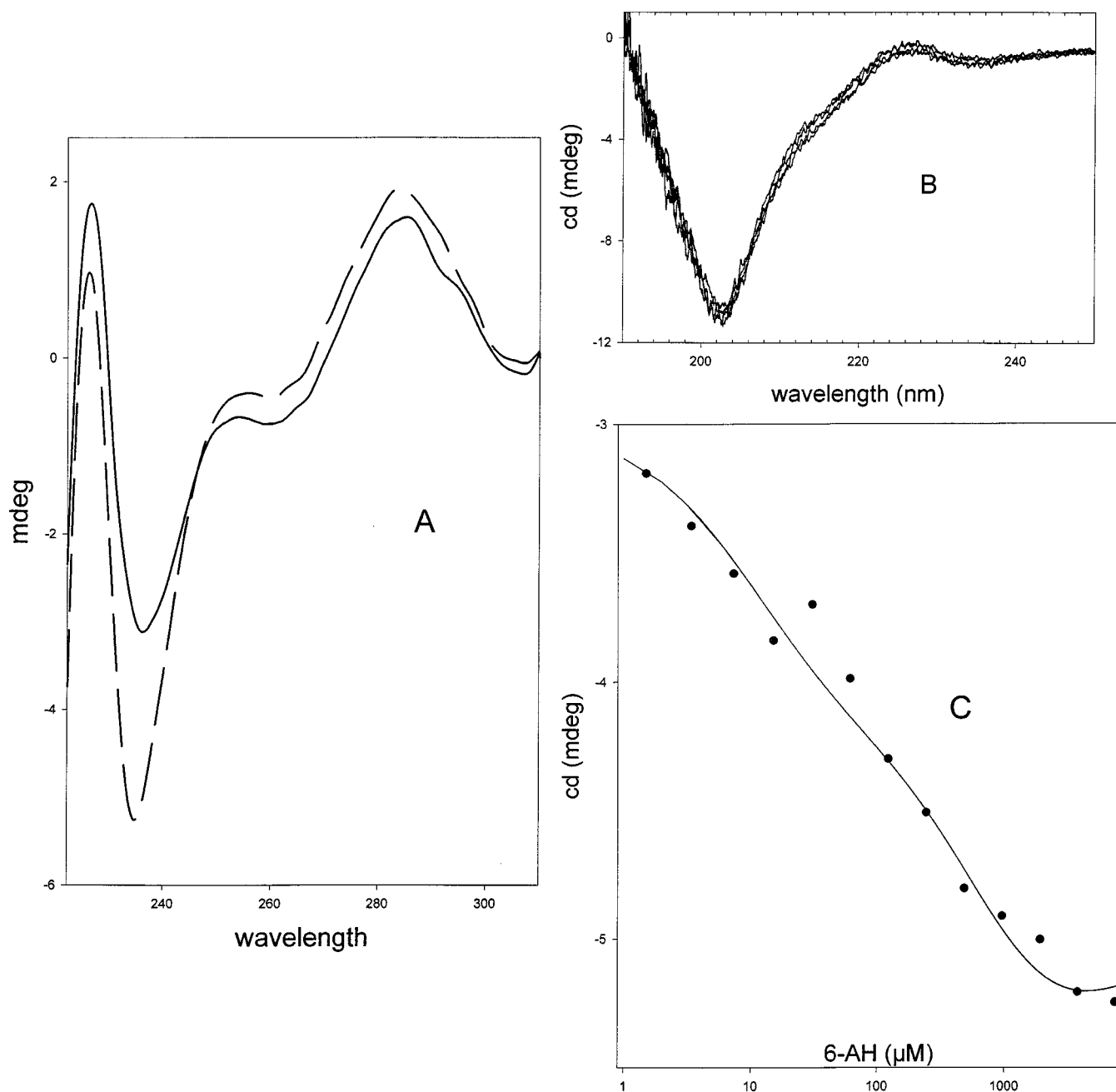


FIGURE 3: (A) Circular dichroic spectra of glu-DPGN from 310 to 220 nm. The solid curve is for glu-DPGN without 6-AH, whereas the dashed curve is for glu-DPGN with 7.6 mM 6-AH. The buffer was 10 mM phosphate (pH 6.8); $T = 288$ K. The positive band at 295 nm and the negative band at 235 nm are characteristic of tryptophan. (B) The CD response of glu-DPGN to 6-AH in the far-UV region. The lowest concentration of 6-AH was 0.5 μ M, and the concentration was increased in two steps to a final concentration of 7.6 mM. There was no significant difference between any of the curves in the far-UV region. (C) The variation of the CD signal at 235 nm as a function of 6-AH concentration. The data were fit to the dissociation coefficients shown in Figure 1 (—). The $\Delta\epsilon$ values were evaluated using the same fitting routine as in the fluorescence experiments. Black circles are the data points. The data are shown as a log-linear plot to allow the viewer to see the stepwise nature of the titration.

B concentrates on the far-UV region. There are several significant aspects of the spectra. First is the fact that the tryptophan shoulder at 295 nm, which shows up as a small band with positive ellipticity in the sample without 6-AH, is not present in the sample that contains a high concentration of 6-AH. While the data are not shown, the response is graded over the titration range of from 0 to 25 mM. The major change in the spectrum occurs in the far-UV contribution of tryptophan (220–240 nm). The magnitude of the negative band decreases by a factor of $\sim 30\%$; this band is relatively broad and spills over at 225 nm such that there is

a small decrease in intensity at the latter wavelength. In the far-UV region, between 220 and 190 nm, there is absolutely no detectable change in ellipticity resulting from the addition of 6-AH (panel B). Since the absorption bands in the far-UV region are primarily the result of secondary structure and ordering of the peptide bond, the conclusion is obvious and must be stated: The very large change in conformation exhibited by DPGN on addition of 6-AH is not the result of large-scale changes in secondary structure.

In Figure 3C, we show the results of the titrations of Figure 3A in which the change in ellipticity at 235 nm as a function

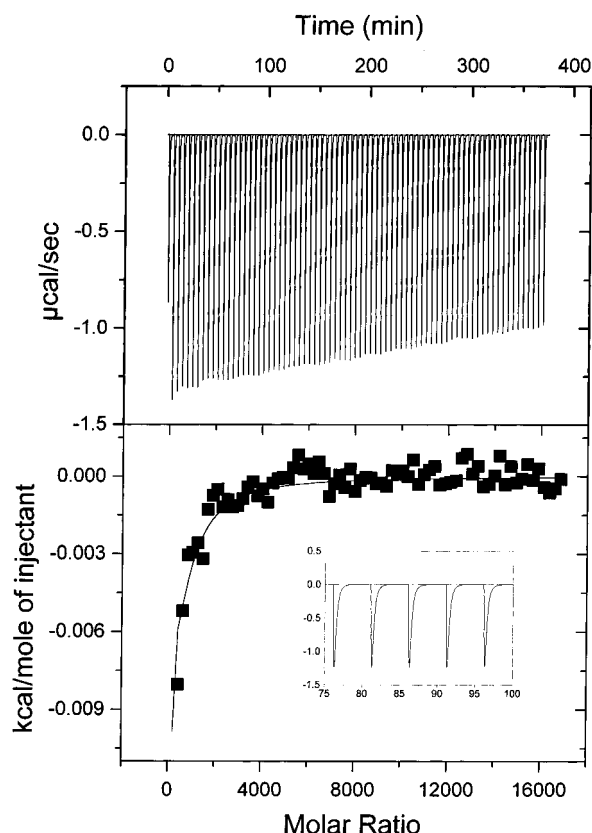


FIGURE 4: Isothermal titration calorimetry of glu-DPGN. The initial concentration of glu-DPGN was $2 \mu\text{M}$; the concentration of 6-AH in the injection syringe was $\sim 500 \text{ mM}$. The temperature was maintained at 288 K . (Top) The actual heat changes occurring during the injection sequence; an expanded view of the data is shown in the inset of the bottom panel. (Bottom) The enthalpic changes as a function of the molar ratio of ligand to protein. The non-zero baseline has been subtracted from the data in the bottom panel. The black squares are the actual heat changes; the solid line is the data fit to the association constants obtained in Figure 1. The calculated enthalpies and entropies are given in Table 1.

of 6-AH concentration has been plotted. Once again, the solid points are the actual data. The data were then fit using the regression function of Sigma Plot to extract values for the extinction coefficients associated with each dissociation coefficient. The solid line represents data fitted on the basis of the dissociation coefficients of Figure 1 in conjunction with the extinction coefficients. As was the case for the fluorescence data, the fits are quite acceptable. The data of Figure 3C are presented as a linear-log plot to emphasize the stepwise nature of the curve (29, 30).

Figure 4 shows the results of an isothermal titration calorimetric run in which glu-DPGN was titrated with 6-AH. The top portion of the figure shows the raw heat data from the run. The bottom portion shows the enthalpy changes as a function of the ratio of ligand to plasminogen after subtraction of the sloping baseline. Using the software supplied by Microcal, there was no unique fit to the data. When we applied the dissociation constants of Figure 1 (expressed as association constants) to the data, we obtained the fit shown by the solid line through the data. The enthalpies and calculated entropies are shown in Table 1. The most striking thing about the thermodynamic values is that the enthalpies are all negative but range from -0.5 kcal/mol for the tight sites to -11 kcal/mol for the weakest site. The entropies for

Table 1: Binding of 6-AH to Individual Sites of Canine Plasminogen

association constants and thermodynamic constants for binding sites in DPGN ^a	glu-plasminogen	lys-plasminogen
$K_{a1} (\text{M}^{-1})$	1.4×10^5	2.7×10^5
$\Delta G_1 (\text{kcal/mol})$	-6.8	-7.1
$\Delta H_1 (\text{kcal/mol})$	-0.45	-0.075
$\Delta S_1 (\text{cal mol}^{-1} \text{K}^{-1})$	22	25
$K_{a2} (\text{M}^{-1})$	6.6×10^4	5×10^4
$\Delta G_2 (\text{kcal/mol})$	-6.4	-6.2
$\Delta H_2 (\text{kcal/mol})$	-0.45	-0.075
$\Delta S_2 (\text{cal mol}^{-1} \text{K}^{-1})$	20	21
$K_{a3} (\text{M}^{-1})$	1.17×10^3	1.4×10^3
$\Delta G_3 (\text{kcal/mol})$	-4	-4.1
$\Delta H_3 (\text{kcal/mol})$	-2.2	-1.5
$\Delta S_3 (\text{cal mol}^{-1} \text{K}^{-1})$	6.3	9.3
$K_{a4} (\text{M}^{-1})$	2.5×10^2	2.3×10^2
$\Delta G_4 (\text{kcal/mol})$	-3.2	-3.1
$\Delta H_4 (\text{kcal/mol})$	-11	-0.21
$\Delta S_4 (\text{cal mol}^{-1} \text{K}^{-1})$	-25	10

^a The data have been rounded off to two significant figures. As a result, the sum of ΔH and $T\Delta S$ do not always equal ΔG .

all but the weakest site are positive. $-T\Delta S$ is evaluated to be approximately -6 kcal/mol for the two tightest sites, -2 kcal/mol for site 3, and 8 kcal/mol for the weakest site. The driving force for 6-AH binding to the weakest site is clearly enthalpy. This result is quite unexpected.

Lys-plasminogen lacks the N-terminal peptide containing lysine 50. It is known to exist in an open conformation not identical with that of 6-AH-opened plasminogen but similar (4) (see the Discussion). Fluorescence titrations were carried out using the same protocols as described in the legends of Figures 1 and 2. The data are shown in panels A and B of Figure 5. As was the case with glu-plasminogen, the decrease in fluorescence is followed by an increase. When the data were fit to the sum of four hyperbolas, the fits were virtually as good as those for the glu-plasminogen. The eight constants were not the quite the same in the two preparations; the values for the lys-plasminogen are shown in the figure. The major change occurs in the K_d for the weakest site. It decreases from 4 to 3 mM. The binding of 6-AH for this site is marginally tighter in the lys-plasminogen than in glu-plasminogen.

The calorimetric response of lys-plasminogen on titration with 6-AH is different from that of the holoenzyme (Figure 6 and Table 1). The experiments whose results are depicted in Figure 6 were similar to those of Figure 4, and the two panels have the same significance. In the lower panel, the line drawn through the data was based on the dissociation constants of Figure 5. As can be seen from the comparison of the two forms of DPGN in Table 1, the first three binding sites do not change substantially. There is a major change that occurs in site 4 associated with kringle 5. ΔS reverses sign and goes from -25 to $10 \text{ cal mol}^{-1} \text{K}^{-1}$. ΔH increases from -11 to -3.3 kcal/mol . This means that the binding of 6-AH to kringle 5, when it is not an exchange reaction, is similar to the binding to the other kringles; the reaction is entropy-driven to the same extent as it is in the other kringles.

DISCUSSION

In this work, we used fluorescence to detect the binding of 6-AH to canine plasminogen. We previously used this

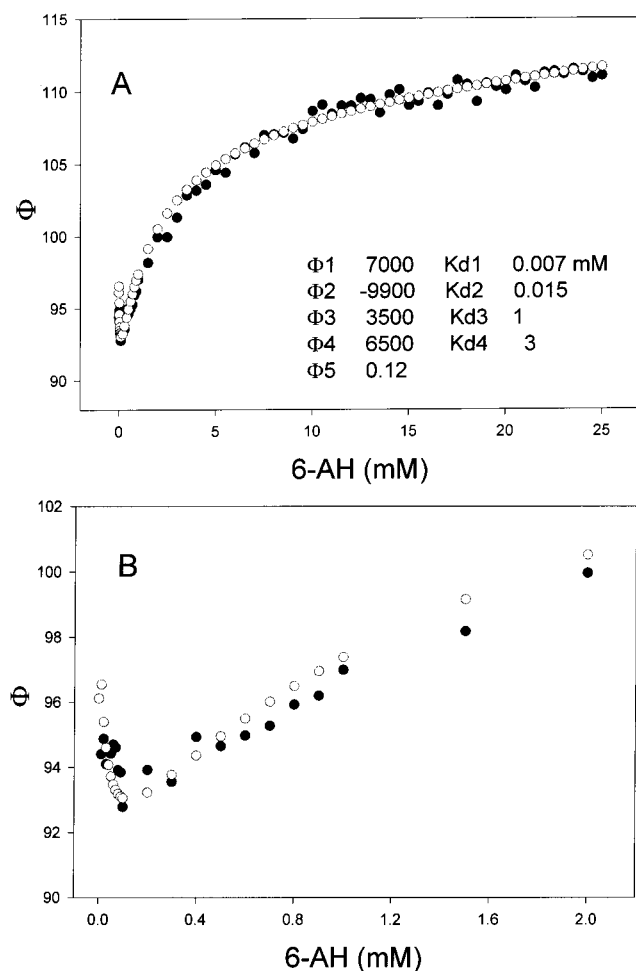


FIGURE 5: (A) Intrinsic fluorescence response of lys-DPGN to 6-AH. The data were evaluated using the equation shown in the Results. The concentration of lys-DPGN was 2 μ M; the concentration of 6-AH varied from 10 μ M to 25 mM. The black circles are the actual data points; the white circles are data fit to the equation shown in the Results. $T = 288$ K. The buffer contained 25 mM Mes, 25 mM Tris, 1 mM Mg(OAc)₂, and 0.1 mM EDTA (pH 6.5). The fluorescence coefficients and the dissociation coefficients are given in the inset. (B) The same data but emphasizing data between 10 μ M and 2 mM 6-AH.

approach to dissect out the binding constants of human plasminogen (31). The two proteins, canine and human, are very similar. They have tryptophans at identical positions in kringles 4 and 5 and the catalytic domain. The sequences of the other three canine kringles are not known; there are no tryptophans in the NTP (26, 27).

We have presented data that relate to the thermodynamics of the interaction of canine plasminogen and 6-aminohexanoate. The final thermodynamic parameters are based entirely on binding constants and a model derived from the fluorescence measurements. The fluorescence data are clear. Fluorescence decreases at 6-AH concentrations between 0 and 0.1 mM 6-AH. At higher concentrations, the fluorescence increases.

The fluorescence increase occurs with a slope that indicates that it has a midpoint in the millimolar range. It has been well established by Castellino, Christensen, Markus, and Ponting as well as many other groups that opening of plasminogen occurs when the concentration of 6-AH is above the millimolar range.

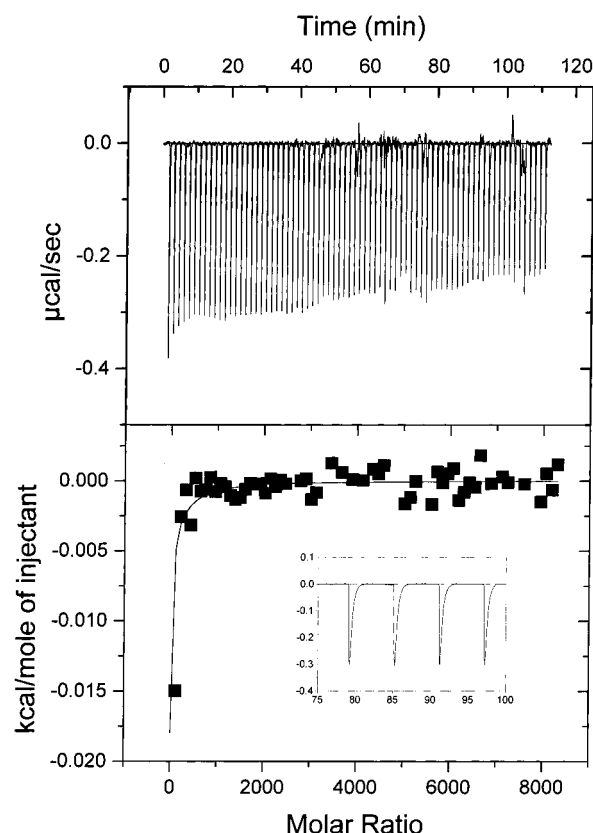


FIGURE 6: Isothermal titration calorimetry of lys-DPGN. The initial concentration of lys-DPGN was 2 μ M; the concentration of 6-AH in the injection syringe was \sim 500 mM. The temperature was maintained at 288 K. (Top) The actual heat changes occurring during the injection sequence; an expanded view of the data is shown in the inset of the bottom panel. (Bottom) The enthalpic changes as a function of the molar ratio of ligand to protein. The non-zero baseline has been subtracted from the data in the bottom panel. The black squares are the actual heat changes; the solid line is the data fit to the association constants obtained in Figure 5. The calculated enthalpies and entropies are given in Table 1.

The isolated human kringles have been studied. The studies show quite clearly that the kringles containing three tryptophans (kringles 2 and 4) exhibit positive fluorescence changes when they bind 6-AH. Kringles 1 and 5 (each containing two tryptophans) exhibit negative changes when they bind the ligand. A partial explanation for this is given in ref 31. There are at least four kringles in plasminogen that bind 6-AH. Presumably, the fifth kringle also binds but with an affinity that is too low to detect using current methods. The binding of 6-AH to both human (31) and canine plasminogen can be modeled as the sum of four independent binding reactions. We assigned the binding order on the basis of the sign of the fluorescence deflection, the magnitude of the calculated K_d , and the fact that kringle 5 is thought to be the predominant internal ligand for the NTP. However, there are four kringle binding domains, each with its own fluorescence response. There is no unique solution to the binding using only the data obtained from the fluorescence titration. This is the major weakness in our approach. The major strength of the approach is that all the fluorescence, CD, and calorimetric data can be well modeled using the same dissociation coefficients. Our binding order is as follows: kringle 4 binding which is tighter than kringle

Table 2: Binding of 6-AH to Human and Canine Plasminogen^a

	kringle 1	kringle 2	kringle 3	kringle 4	kringle 5
K_d for HPGN	12 μ M	0.52 mM	does not bind	4 μ M	1.6 mM
K_d for DPGN	15 μ M	0.85 mM		7 μ M	4 mM
Φ for HPGN	-6.4	1		1	9.2
Φ for DPGN	-2.1	1		1.3	1.2

^a A comparison of the dissociation constants and normalized fluorescence coefficients. The assignment of the dissociation constants and the fluorescence coefficients is based on the sign of the fluorescence change of the isolated human kringles and the approximate dissociation constants of the isolated kringles. The probable reason for the positive and negative changes in fluorescence that occur on ligand binding is described in detail in ref 31. The dissociation constants for the two proteins are quite similar. The relative fluorescence coefficients differ considerably in absolute magnitude but not in sign. Titration of human plasminogen leads to a very large decrease in fluorescence which then recovers to even greater positive values.

1 binding which is tighter than kringle 2 binding which is tighter than kringle 5 binding.

Isolated kringle 4 has a positive fluorescence change when binding 6-AH and a very tight binding constant. Kringle 1 has a negative change and a very tight binding constant. Because of the sign of the fluorescence change, we cannot successfully model the binding if we reverse the affinities of kringles 1 and 4. Our assignments of K_d values for kringles 4 and 1 differ from that based on the literature. As isolated, kringle 1 ($K_d = 12 \mu$ M) binds 6-AH about twice as tightly as kringle 4 ($K_d = 26 \mu$ M). This represents a difference in binding energies of <0.5 kcal/mol, less than the energy contributed by a weak hydrogen bond. Similarly, the order we assign to the two K_d values results in binding energies that differ by less than 0.5 kcal. To go from the assignments in the isolated human kringles to that in the intact dog plasminogen requires a change in kringle 4 of ~ 0.75 kcal/mol, the energy associated with a change in one hydrogen bond. The K_d of isolated kringle 2 and our assignment agree. Kringle 5 is assigned the final binding site because it is the predominant site for the NTP. Our K_d values do not differ significantly from those of the isolated kringles except in the case of kringle 5 where the reported K_d is $\sim 140 \mu$ M and the value we report is ~ 20 times that value. What accounts for the difference? In the absence of subangstrom structural data on the complete protein, there is no explanation. We note however that no one (as far as we know) disagrees with the fact that the final binding of 6-AH involves a site with a dissociation constant in the millimolar range.

The binding reactions have been fit to the sum of four simple binding curves of the type $K_d = (a)(b)/(ab)$ or $K_a = (ab)/(a)(b)$. The binding constants so obtained are similar to those obtained for the same ligand binding to human plasminogen (Table 2). The latter figures have been assembled for the individual human kringles by Marti et al. (32) and more recently for intact human plasminogen (31). The overall picture of the fluorescence data on the intact plasminogen presented here differs from that presented by other investigators in the past. Whereas many studies have invoked cooperative effects between sites (33), our data, for both human and canine plasminogen, show no indication that cooperativity is operating in the binding and resultant conformational change. Cooperativity (29, 30) is taken to mean that binding at an allosteric site influences the overall conformational change studied here. Until now, the only data

that have supported the view that cooperative effects are operative come from studies of intrinsic tryptophan fluorescence (24, 33); where both intrinsic tryptophan fluorescence and extrinsic fluorescence from a probe at the active site have been studied, the extrinsic fluorescence responds in a noncooperative fashion (24). We find no evidence for cooperativity in either the fluorescence or CD data. On the contrary, both sets of data indicate simple binding phenomena. Others have found evidence for cooperative effects. We attribute the difference between other studies and ours to the fact that the data shown in Figures 1 and 2 are far more extensive than most. We are able to detect and quantify binding to the tightest sites. One of these has a negative fluorescence response on binding 6-AH. When the data are not sufficiently extensive, the negative change for binding to the second tightest site sums with the positive change of the other two tight sites to yield what appears to be a sigmoid type curve; it is an artifact of having too few points in the region of tight binding. With the exception of one kinetic study by Christensen and Mølgaard (34), other studies have missed the decrease in fluorescence when 6-AH binds. Needless to say, the absence of data indicating cooperative effects cannot in any way be taken to mean that there are no cooperative effects operating.

The conclusions vis-à-vis cooperativity are reinforced when viewing the CD data between 295 and 235 nm. Over a 1000-fold range in concentrations, there is no evidence for cooperative interactions occurring in the binding of 6-AH or the opening of the DPGN. In the far-UV region of the spectrum (220–190 nm), there is no evidence for any change in the secondary structure of the protein. Given that, the structure of the protein changes. There is no question that it goes from a closed form to an open form on addition of sufficient 6-AH. There is also no question but that this can be accomplished by rotation about relatively few bonds. One can envisage DPGN, in the absence of added ligand, as a weak spring of 100 peptide bonds decorated with five kringles. The spring is bent back on itself, and the hasp of the spring is formed from the interaction of lysine 50 and kringle 5. The equilibrium is displaced by addition of 6-AH which causes the hasp to weaken. We speculate that the new Ψ and Φ angles associated with the peptide bonds are much the same as the old with a few exceptions. It is not surprising that no difference is seen in the far-UV CD. There are after all more than 700 peptide bonds that contribute to the spectrum in the far-UV region.

There are major changes in the CD spectrum at 235 nm. These probably result from slight changes in the environments of the 10 tryptophans located in the four kringles that bind 6-AH. The entire protein contains only ~ 19 tryptophans. The tryptophan CD spectrum is exquisitely sensitive to environment in the 230 nm region and has been shown to change with ionic composition, solvent, and lipid proximity (35, 36). On the basis of the X-ray and NMR structures of the isolated kringles, there is little doubt that the immediate environments of these tryptophans change even if their orientations in the ligated and free states remain more or less the same.

The thermodynamic data are somewhat more perplexing. The X-ray and NMR structures of the individual kringles indicate that there is little room in the binding sites for both water and ligand (7–12). When water is released from either

the binding site or the ligand, it enters the bulk phase with the resultant gain in entropy; accordingly, we expect that entropy should be the driving force of 6-AH binding. The binding of 6-AH to the two tightest sites of intact DPGN follows the expected pattern. However, it is not the result obtained for binding to isolated human kringle 1 (37), 2 (38), and 4 (39); these correspond to sites 2, 3, and 1, respectively, in Table 1. In the case of kringle 2, the data from this study show much the same trend as those on the isolated kringle; the driving force for binding is divided between ΔH and ΔS (38). In the case of kringle 1 and 4, our binding constants are about the same as theirs; ΔS and ΔH differ substantially. At this point, it is unclear whether the difference is due to dog versus human or isolated kringle versus intact plasminogen; certainly, there are differences in the response of the proteins of the two species (*vide infra*). The binding of 6-AH to the loose site on kringle 5 is more problematic. In this case, binding of 6-AH displaces lysine 50. The 6-AH becomes dehydrated while lysine 50 is hydrated. There is little or no change in the hydration state of the binding pocket. The prediction, based on just the change in hydration of binding pockets and substrates, is that binding to kringle 5 should be driven less by entropy than by the other three binding kringles; this must be true if one considers only the binding reaction independent of the conformational change. The problem arises when one considers that this exchange reaction breaks the noncovalent interaction between kringle 5 and the NTP. The molecule simultaneously undergoes the large conformational change. One would have anticipated that the loss of conformational constraint would result in a large entropy change, but this does not appear to be the case. There is an overall loss of entropy for kringle 5 exchanging 6-AH for lysine 50 which results in a $-T\Delta S$ that is positive. The combined exchange reaction is dominated by the -11 kcal/mol enthalpy.

If one compares the weakest dissociation constant of glu-plasminogen binding 6-AH and that of the isolated kringle 5, one finds that they are not the same. Glu-DPGN binds 6-AH much more weakly than does the isolated kringle. The change in binding constants can be used to determine the extent to which glu-DPGN is in the open conformation when no added ligand is present. The approach is detailed by Kornblatt (31) but relies on the fact that the ratio of the constants yields the position of the closed–open equilibrium:

$$K_{\text{d(appeant for glu-DPGN)}} = K_{\text{d(appeant for kringle 5)}} K_{\text{eq(closed/open for glu-DPGN)}}$$

Since $K_{\text{d(appeant for glu-DPGN)}}$ is ~ 4 mM and $K_{\text{d(appeant for kringle 5)}}$ is ~ 0.14 mM, $K_{\text{eq(closed/open for glu-DPGN)}}$ is determined to be ~ 28 . In the absence of added ligand, the closed–open equilibrium is set to favor the closed form more than the open form. The human protein exhibits similar behavior; the closed form is favored by a factor of 3–20 (31).

If one compares glu- and lys-plasminogen, one finds that the dissociation constants for 6-AH binding to kringle 5 in the intact proteins are almost the same. This is a disturbing result; if there were only two plasminogen states, open and closed, the K_d of lys-PGN binding 6-AH should be about the same as that of isolated kringle 5 binding 6-AH. In HPGN, this situation approximately applies (16); one finds that the dissociation constant for one of the weak sites

decreases (gets tighter) by a factor of ~ 20 when the NTP is cleaved off. This is not occurring here with DPGN. We interpret the similar K_d values in the two dog proteins to indicate that we are not dealing with a single equilibrium but rather with a complex of equilibria (2–4, 19, 40–43) in lys-DPGN. Removal of the NTP allows kringle 5 to establish other equilibria in which the kringle is either associated with other ligands or otherwise shielded from 6-AH. This additional conformational state clearly complicates the analysis for lys-DPGN; it is much less important for our analysis of the glu-DPGN data.

The enthalpic changes that occur on binding and opening of glu-plasminogen indicate that the open form is more hydrated than the closed form. Furthermore, when the NTP is cleaved off, as in the case of lys-plasminogen, the binding of 6-AH to kringle 5 is driven by entropy as is the case with the other three kringles. This indicates to us that the major portion of the conformational change itself must be associated with a substantial change in hydration of the protein. The prediction is that DPGN should open when exposed to high hydrostatic pressure. Pressure acts by promoting the hydration of hydrophobic and polar surfaces, the electrostriction of ionized groups, and the collapse of small voids that result from poor packing of the protein. The latter need not concern us here. What is important is that hydrostatic pressure does promote opening of the protein in the absence of an added ligand such as 6-AH. Water can act as an alternative ligand for kringle 5. The driving force here must be hydration of the kringle 5 binding pocket, electrostriction of the amino group of lysine 50, and hydration of substantial portions of buried protein as DPGN opens. We showed (22) that electrostriction and hydration of the kringle 5 binding pocket could account for about half of the 30 mL/mol volume change associated with the pressure-induced opening of the molecule. The remainder of the change must be associated with hydration of the protein as it opens. The response of the protein to osmotic pressure should indicate the number of waters associated with this change. Unfortunately, plasminogen exhibits preferential binding of small osmolytes (J. A. Kornblatt, unpublished) such that we cannot make measurements in “disperse solution” (44, 45) as we have done in the past. This complicates the nature of experiments that must be carried out but by no means precludes them.

REFERENCES

1. The National Institute of Neurological Disorders and Stroke rt-PA Stroke Study Group (1995) *N. Engl. J. Med.* 333, 1581–1587.
2. Ponting, C. P., Marshall, J. M., and Cederholm-Williams, S. A. (1992) *Blood Coagulation Fibrinolysis* 3, 605–614.
3. Cockell, C. S., Marshall, J. M., Dawson, K. M., Cederholm-Williams, S. A., and Ponting, C. P. (1998) *Biochem. J.* 333, 99–105.
4. Marshall, J. M., Brown, A. J., and Ponting, C. P. (1994) *Biochemistry* 33, 3599–3606.
5. An, S. S., Carreno, C., Marti, D. N., Schaller, J., Albericio, F., and Llinas, M. (1998) *Protein Sci.* 7, 1960–1969.
6. Chang, Y., Mochalkin, I., McCance, S. G., Cheng, B., Tulinsky, A., and Castellino, F. J. (1998) *Biochemistry* 37, 3258–3271.
7. Mathews, I. I., Vanderhoff-Hanaver, P., Castellino, F. J., and Tulinsky, A. (1996) *Biochemistry* 35, 2567–2576.
8. Wu, T. P., Padmanabhan, K. P., and Tulinsky, A. (1994) *Blood Coagulation Fibrinolysis* 5, 157–166.

9. Wu, T. P., Padmanabhan, K. P., Tulinsky, A., and Mulichak, A. M. (1991) *Biochemistry* 30, 10589–10594.
10. Mulichak, A. M., Tulinsky, A., and Ravichandran, K. G. (1991) *Biochemistry* 30, 10576–10588.
11. Wang, X., Lin, X., Loy, J. A., Tang, J., and Zhang, X. C. (1998) *Science* 281, 1662–1665.
12. Marti, D. N., Schaller, J., and Llinas, M. (1999) *Biochemistry* 38, 15741–15755.
13. An, S. S., Marti, D. N., Carreno, C., Albericio, F., Schaller, J., and Llinas, M. (1998) *Protein Sci.* 7, 1947–1959.
14. Violand, B. N., Byrne, R., and Castellino, F. J. (1978) *J. Biol. Chem.* 253, 5395–5401.
15. Brockway, W. J., and Castellino, F. J. (1971) *J. Biol. Chem.* 246, 4641–4647.
16. Markus, G., Priore, R. L., and Wissler, F. C. (1979) *J. Biol. Chem.* 254, 1211–1216.
17. Castellino, F. J., Brockway, W. J., Thomas, J. K., Liao, H., and Rawitch, A. B. (1973) *Biochemistry* 12, 2787–2791.
18. Mangel, W. F., Lin, B. H., and Ramakrishnan, K. (1990) *Science* 248, 69–73.
19. Ponting, C. P., Holland, S. K., Cederholm-Williams, S. A., Marshall, J. M., Brown, A. J., Spraggon, G., and Blake, C. C. (1992) *Biochim. Biophys. Acta* 1159, 155–161.
20. Tranqi, L., Prandini, M.-H., and Chapel, A. (1979) *Biol. Cell.* (1977–1980) 34, 39–42.
21. Weisel, J. W., Nagaswami, C., Korsholm, B., Petersen, L. C., and Suenson, E. (1994) *J. Mol. Biol.* 235, 1117–1135.
22. Kornblatt, J. A., Kornblatt, M. J., Clery, C., and Balny, C. (1999) *Eur. J. Biochem.* 265, 120–126.
23. Bachmann, F. (1994) in *Haemostasis and Thrombolysis* (Bloom, A. L., Forbes, C. D., Thomas, D. P., and Tuddenham, E. G. D., Eds.) Vol. 1, pp 575–600, Churchill Livingstone, Edinburgh, U.K.
24. Horrevoets, A. J. G., Pannekoek, H., and Nesheim, M. E. (1997) *J. Biol. Chem.* 272, 2176–2182.
25. Nilsen, S. L., and Castellino, S. J. (1999) *Protein Expression Purif.* 16, 136–143.
26. Schaller, J., and Rickli, E. E. (1988) *Enzyme* 40, 63–69.
27. Schaller, J., Straub, C., Kampfer, U., and Rickli, E. E. (1988) *Protein Sequences Data Anal.* 2, 445–450.
28. Chibber, B. A. K., Deutch, D. G., and Mertz, E. T. (1974) *Methods Enzymol.* 34, 424–431.
29. Bardsley, W. G., and Wyman, J. (1978) *J. Theor. Biol.* 72, 373–376.
30. Wyman, J., and Gill, S. J. (1990) in *Binding and Linkage*, University Science Books, Mill Valley, CA.
31. Kornblatt, J. A. (2000) *Biochim. Biophys. Acta* 1481, 1–10.
32. Marti, D. N., Hu, C.-K., An, S. S. A., von Haller, P., Schaller, J., and Llinas, M. (1997) *Biochemistry* 36, 11591–11604.
33. Christensen, U., and Mølgaard, L. (1992) *Biochem. J.* 285, 419–425.
34. Christensen, U., and Mølgaard, L. (1991) *FEBS Lett.* 278, 204–206.
35. Wallace, B. A. (1987) in *Ion Transport Through Membranes* (Yagi, K., and Pullman, B., Eds.) pp 255–277, Academic Press, New York.
36. Freskgaard, P.-O., Martensson, L.-G., Jonson, B.-H., and Carlsson, U. (1994) *Biochemistry* 33, 14281–14288.
37. Menhart, N., Sehl, L. C., Kelley, R. F., and Castellino, F. J. (1991) *Biochemistry* 30, 1948–1957.
38. Nilsen, S. L., Prorok, M., and Castellino, F. J. (1999) *J. Biol. Chem.* 274, 22380–22386.
39. Sehl, L. C., and Castellino, F. J. (1990) *J. Biol. Chem.* 265, 5482–5486.
40. Horrevoets, A. J. G., Smilde, A. E., Fredenburgh, J. C., Pannekoek, H., and Nesheim, M. E. (1995) *J. Biol. Chem.* 270, 15770–15776.
41. McCance, S., and Castellino, S. J. (1995) *Biochemistry* 34, 9581–9586.
42. Menhart, N., Hoover, G. J., McCance, S., and Castellino, S. J. (1994) *Biochemistry* 33, 1482–1488.
43. Mølgaard, L., Ponting, C. P., and Christensen, U. (1997) *FEBS Lett.* 405, 363–368.
44. Parsegian, V. A., Rand, R. P., and Rau, D. C. (2000) *Proc. Natl. Acad. Sci. U.S.A.* 97, 3987–3992.
45. Timasheff, S. N. (1998) *Proc. Natl. Acad. Sci. U.S.A.* 95, 7363–7367.

BI001857B